



# The Effects of MicroRNAs on Cardiomyopathy in a Rat Model of Streptozotocin-induced Diabetes Mellitus

## Streptozotocin ile İndüklenen Diabetes Mellitus Sıçan Modelinde MikroRNA'ların Kardiyomiyopati Üzerine Etkileri

Aslıhan Şeyda DOĞAN<sup>1,2</sup>, Mukaddes PALA<sup>3</sup>, Şenay GÖRÜCÜ YILMAZ<sup>4</sup>, Ayfer BECEREN<sup>5</sup>, Aydın KARABULUT<sup>6</sup>, Yalçın POLAT<sup>7</sup>, Hatice Kübra ELÇİOĞLU<sup>2</sup>

<sup>1</sup>Biruni University Faculty of Medicine, Department of Medical Pharmacology, Istanbul, Türkiye

<sup>2</sup>Marmara University Faculty of Pharmacy, Department of Pharmacology, Istanbul, Türkiye

<sup>3</sup>Malatya Turgut Özal University Faculty of Medicine, Department of Physiology, Malatya, Türkiye

<sup>4</sup>Gaziantep University Faculty of Health Sciences, Department of Nutrition and Dietetics, Gaziantep, Türkiye

<sup>5</sup>Marmara University Faculty of Pharmacy, Department of Pharmaceutical Toxicology, Istanbul, Türkiye

<sup>6</sup>University of Health Sciences Türkiye, Hamidiye Health Science Institute, Department of Immunology, Istanbul, Türkiye

<sup>7</sup>Biruni University Faculty of Medicine, Department of Pathology, Istanbul, Türkiye

### ABSTRACT

**Objective:** Diabetic cardiomyopathy (DCM) is characterized by complex pathophysiological events. miRNAs play a role in the DCM. In our study, the potential of miRNAs as a biomarker in the diagnosis and treatment of DCM was evaluated in the diabetes model induced by streptozotocin in rats.

**Methods:** Therefore, miRNAs obtained from rat heart tissue were analyzed by microarray, and twelve miRNAs (rno-miR-200c-3p, rno-miR-129-5p, rno-miR-150-3p, rno-miR-3584-5p, rno-miR-34c-3p, rno-miR-342-3p, rno-miR-466b-3p, rno-miR-466c-3p, rno-miR-31a-3p, rno-miR-15b-5p, rno-miR-196b-3p, and rno-miR-208a-5p) with changed expression levels were validated by real-time polymerase chain reaction analysis.

**Results:** As a result of the validation, it was determined that three miRNAs (rno-miR-15b-5p, rno-miR-196b-3p, and rno-miR-208a-5p) were downregulated, one miRNA (rno-miR-200c-3p) was upregulated ( $p < 0.05$ ). MiR-15b-5p, miR-196b-3p, miR-200c-3p, and miR-15b-5p are involved in the regulation of DCM, and the *GRAP2* gene is one of the possible targets of these miRNAs.

**Conclusion:** miR-200c-3p has diagnostic value and may be a biomarker candidate.

**Keywords:** Diabetic cardiomyopathy, miRNA expression, biomarker, streptozotocin

### ÖZ

**Amaç:** Diyabetik kardiyomiyopati (DKM), karmaşık patofizyolojik olaylarla karakterizedir. miRNA'lar DKM'de rol oynamaktadır. Çalışmamızda sıçanlarda streptozotocin ile oluşturulan diyabet modelinde miRNA'ların DKM'nin tanı ve tedavisinde biyobelirteç olarak potansiyeli değerlendirildi.

**Yöntemler:** Bu nedenle, sıçan kalp dokusundan elde edilen miRNA'lar mikroarray ile analiz edildi ve on iki miRNA'nın (rno-miR-200c-3p, rno-miR-129-5p, rno-miR-150-3p, rno-miR-3584-5p, rno-miR-34c-3p, rno-miR-342-3p, rno-miR-466b-3p, rno-miR-466c-3p, rno-miR-31a-3p, rno-miR-15b-5p, rno-miR-196b-3p ve rno-miR-208a-5p) değişen ekspresyon seviyeleri gerçek zamanlı polimeraz zincir reaksiyonu analizi ile doğrulandı.

**Bulgular:** Doğrulama sonucunda, üç miRNA'nın (rno-miR-15b-5p, rno-miR-196b-3p ve rno-miR-208a-5p) downregüle olduğu ve bir miRNA'nın (rno-miR-200c-3p) upregüle olduğu belirlendi ( $p < 0.05$ ). miR-15b-5p, miR-196b-3p, miR-200c-3p ve miR-208a-5p, DKM'nin düzenlenmesinde yer almakta ve *GRAP2* geni, bu miRNA'ların olası hedeflerinden biridir.

**Sonuç:** miR-200c-3p tanısal değere sahiptir ve biyobelirteç aday olabilir.

**Anahtar Kelimeler:** Diyabetik kardiyomiyopati, miRNA ekspresyonu, biyobelirteç, streptozotocin

**Address for Correspondence:** Mukaddes Pala, Malatya Turgut Özal University Faculty of Medicine, Department of Physiology, Malatya, Türkiye  
E-mail: mukaddes.pala@ozal.edu.tr ORCID ID: orcid.org/0000-0002-0610-0526

Received: 25.05.2024  
Accepted: 06.09.2024  
Published date: 27.01.2025

**Cite this article as:** Doğan AŞ, Pala M, Görücü Yılmaz Ş, Beceren A, Karabulut A, Polat Y, Elçioğlu HK, The effects of MicroRNAs on cardiomyopathy in a rat model of streptozotocin-induced diabetes mellitus. Bezmialem Science. 2025;13(1):35-44



©Copyright 2025 by Bezmialem Vakıf University published by Galenos Publishing House.  
Licensed by Creative Commons Attribution-NonCommercial-NoDerivatives 4.0 (CC BY-NC-ND 4.0)

## Introduction

Diabetic cardiomyopathy (DCM) is characterized by diastolic relaxation abnormalities in its early stages and later by dyslipidemia, hypertension, and heart failure (1). Insulin resistance, hyperinsulinemia, and hyperglycemia are independent risk factors for the development of DCM (2). Systemic metabolic disorders, inappropriate activation of the renin-angiotensin-aldosterone system, subcellular component abnormalities, oxidative stress, inflammation, and dysfunctional immune modulation can lead to the development of DCM (3). These abnormalities promote cardiac tissue interstitial fibrosis, heart stiffness/diastolic dysfunction, and then systolic dysfunction, precipitating heart failure (4). The dysregulation of coronary endothelial cells and exosomes contribute to the pathology of DCM (5). Interstitial fibrosis, myocyte hypertrophy, and increased contractile protein glycosylation in heart tissue are seen in DCM (6). Systolic and diastolic dysfunction is observed in patients with DCM (7).

Mitogen-activating protein kinases (MAPKs) signaling pathway is dysregulated in DCM (8). Increased activity of MAPKs has been demonstrated in the streptozotocin (STZ)-induced diabetes model (9).

miRNAs are highly expressed in the cardiovascular system and may play a role in cardiovascular development and diseases (10). miRNAs regulate gene expression by inhibiting translation or allowing mRNA to be degraded (11).

The GRB2-related adapter protein 2 (GRAP2) is a member of the GRB2/Sem5/Drk family. This protein is involved in leukocyte-specific protein tyrosine kinase signaling (<https://www.genecards.org/cgi-bin/carddisp.pl?gene=GRAP2>). In cardiac hypertrophy, it manifests itself with an increase in response to pressure overload against mechanical stress. GRAP2 performs this function by activating MAPK through RAS, ROS, and other signaling molecules. GRAP2 regulates fibrosis, fetal gene induction, and cardiomyocyte growth (12). Adapter proteins regulate insulin signaling in diabetic patients work in coordination with substrates such as GRAP2 and increase IRS2 phosphorylation. The uptake of GRAP2, which is an obstacle to maintaining the balance between cell death and survival, is inhibited, insulin signaling is impaired, and the diabetic neuropathy process is contributed (13). The ability of GRAP2 to be regulated by miRNAs is an important target both in terms of understanding its potential in diseases and terms of its diagnostic value.

In this study, the expression levels of DCM-related miRNAs were determined in the STZ-induced diabetes model. Additionally, target genes and signaling pathways of miRNA were identified by bioinformatic analysis.

## Methods

### Animals and Experimental Modeling of Diabetes

Fifteen male Sprague Dawley rats (300-400 g) were used. The rats were obtained from Marmara University Experimental

Animal Research Center. Rats were kept under controlled temperature ( $22 \pm 1 \text{ }^\circ\text{C}$ ) and humidity (60%) conditions on a 12-hour light/dark cycle with access to food and water. Rats were divided into two groups; diabetes ( $n=9$ ) and control ( $n=6$ ). The rats were given a single i.p. injection of 60 mg/kg streptozotocin (STZ; Sigma, St. Louis, MO) in 10 mM sodium citrate (Sigma, St. Louis, MO) buffer (pH 4.6) (14). Two days after the STZ injection, blood glucose levels were measured with an Accu-Chek Go (Roche) glucometer. Rats with blood glucose levels above 200 mg/dL were considered diabetic. After 6 weeks, the weights of the rats were measured. Intracardiac blood was drawn from the anesthetized rats, and the heart tissues were removed. The left ventricle of the heart was dissected and stored at  $-80 \text{ }^\circ\text{C}$  for gene expression analysis. A portion of the left ventricle was taken in 10% formaldehyde for histological analysis.

### RNA Extraction Procedure

Homogenization was performed by adding 50 mg of heart tissue and 450  $\mu\text{L}$  of lysis buffer solution to tubes with ceramic beads. Total RNA isolation was performed according to the kit (GenUP™ Total RNAKit-biotechrabbit) protocol. RNA purity and quantification were performed with a spectrophotometer (Thermo Scientific™ NanoDrop™ 2000, Massachusetts, USA). The RNA pool was created by mixing an equal amount of RNA from the heart tissues of rats in diabetes and control groups in an equal amount of 100 ng/ $\mu\text{L}$  in a tube for each group.

### Microarray Profiling of miRNAs

The Affymetrix GeneChip microRNA 4.0 Array was used to analyze miRNA expressions (Ay-ka Limited Company). In this array, 1,250 miRNAs belonging to *Rattus norvegicus* species were screened and 2-fold or more changes were detected in 81 miRNAs. The 12 most upregulated and most downregulated miRNAs were selected. The criteria for this selection were folded change  $\geq 2$  and  $p < 0.05$ .

### Complementary DNA (cDNA) Analysis

cDNA synthesis was performed from 10 ng total RNA by reverse transcription PCR using the kit (qScript™ microRNA Synthesis Kit- VWR).

### miRNA Expression Analysis

miRNA expression analyses were performed by real-time polymerase chain reaction (RT-PCR). RT-PCR amplifications were performed with Syber Green PCR Master mix (Perfecta® SYBR Green FastMix® Reaction Mixes-VWR, Beverly, California) using the BIORAD-CFX Connect RT-PCR system. Each sample was analyzed in duplicate. For the relative analysis of miRNA expressions in heart tissue, an endogenous control *U6* gene (15) was used. The reaction mixture was prepared as 20  $\mu\text{L}$  total volume, 10  $\mu\text{L}$  2X SYBR Green SuperMix, 0.4  $\mu\text{L}$  advanced primer (Rat U6 for tissue endogenous control), 0.4  $\mu\text{L}$  reverse primer (Universal PCR primer), 8.2  $\mu\text{L}$  nuclease-free water, and 1  $\mu\text{L}$  cDNA. Thermal cycling conditions were programmed for 10 min at  $95 \text{ }^\circ\text{C}$ , followed by 5 seconds at  $95 \text{ }^\circ\text{C}$ , 15 seconds at  $60 \text{ }^\circ\text{C}$ , and 15 seconds at  $70 \text{ }^\circ\text{C}$  40 cycles.

By performing a melting curve analysis in the extension step, RT was programmed to make a reading from 70 °C to 90 °C in 0.2 seconds in 0.5 °C increments. Up and down-regulation of miRNAs using the obtained cDNAs was determined by RT-PCR. Each sample was analyzed in duplicate. Samples were standardized by U6 endogenous control ( $\Delta$ CT). The relative quantification of the standardized samples was calculated by the  $2^{-\Delta\Delta CT}$  method (16).

**Bioinformatic Analysis**

The miRDB database was used to find potential target genes for 4 miRNAs (<http://mirdb.org/cgi-bin/search.cgi>). In selecting target genes, those with miRNA: target gene matching scores between 70% and 100% were preferred. Obtained results were verified with TargetScan 7.2 ([http://www.targetscan.org/vert\\_72/](http://www.targetscan.org/vert_72/)). The common target of these 4 miRNAs was determined to be the *GRAP2* gene. These miRNAs and target genes were searched in CDM by searching the HMDD database (<https://www.cuilab.cn/hmdd>). MiRPathDB (<https://mpd.bioinf.uni-sb.de/mirnas.html?organism=hsa>), Reactome (<https://reactome.org/>), and Kyoto Encyclopedia of Genes and Genomes (KEGG) pathway databases (<https://www.genome.jp/kegg/pathway.html>) was used to detect metabolic pathways involving the *GRAP2* gene. These genes were evaluated in both species using the Human-Mouse: Disease Connection database (<http://www.informatics.jax.org/mgihome/projects/aboutHMDC.shtml>). Finally, because multiple miRNAs target the same gene, the mirDIP database (microRNA Data Integration Portal) was used to identify the target of this miRNA (<http://ophid.utoronto.ca/mirDIP/index.jsp#r>).

**Histological Analysis**

Heart tissues were fixed in 10% formaldehyde and then passed through an increasing alcohol series. Heart tissue was embedded in paraffin and 4  $\mu$ m sections were cut. The slides were treated with hematoxylin eosin, and Masson trichrome stain (Atom Scientific, UK). The samples were examined under a light microscope according to the Kiernan protocol (17) (Nikon Model Eclipse E200MV R and Nikon Digital Imagine Camera). To evaluate histopathological changes in the heart muscle and fibers, slides were graded histopathologically, and “0” was considered negative, “1” mild, “2” moderate, and “3” severe (17).

**Statistical Analysis**

Statistical analysis was performed using Graphpad Prism 5.0 (Graphpad Software, San Diego, Ca, USA). All data were

expressed as mean  $\pm$  standard deviation. One-way analysis of variance (ANOVA) and Tukey’s test were used in the evaluation between the groups. Mann-Whitney U test was used for comparisons between the means of myocyte diameters of groups. p-value was accepted as 0.05. Receiver operating characteristic (ROC) curve was performed, and area under the curve was assessed for the specificity and sensitivity of miRNAs. The data were analyzed using the statistical package SPSS (Release 11.5, SPSS Inc, Chicago, IL, USA) for Windows.

**Results**

Bodyweight measurements and blood glucose values at the beginning of the study and 6 weeks after STZ administration are given in Table 1. At the end of 6 weeks, a significant decrease in body weight and hyperglycemia were observed in the diabetes group. The blood glucose levels of the diabetic rats showed a significant increase compared to the control group.

**Gene Chip microRNA 4.0 Array Analysis**

Twelve miRNA genes, 4 of which were the most upregulated and 8 were the most downregulated genes, were selected. Fold change  $\geq 2$  and  $p < 0.05$  values were used in this selection (Table 2).

**miRNA Expression Analysis**

It was found that miR-200c-3p, miR-15b-5p, miR-196b-3p, and miR-208a-5p showed a significant difference in diabetic rats compared with the control group ( $p < 0.05$ ) (Figure 1). The regulation status of these miRNAs was demonstrated Table 3, Figure 2.

**miRNA Bioinformatics Analysis**

In the target gene analyses for 4 miRNA and DCM, 220 genes for DCM, 36 genes for miR-200c-3p, 3,573 genes for miR-15b-5p, 649 genes for miR-196b-3p, 4786 genes for miR-208a-5p were compared. The *GRAP2* gene was detected in both miRNAs and DCM (Supplement table 1). In the pathway analysis for GRAP2, 4 signal pathways and 11 sub-pathways that could be related to DCM were detected. According to the Reactome database, it was determined that the intercellular signal transduction pathway was receptor tyrosine kinase. Then, 11 effective sub-pathways and signal diagrams were obtained for these signal pathways. Signal diagrams were detected as TCR signaling, Fc epsilon receptor (FCER1) signaling, DAP12 interaction, and FLT3 signaling. The subpathways were identified as FGFR, NTRK2, EGFR, ERBB2, MET, PDGF, IGF12, Insulin receptor, VEGF, EBB4, and SCF-KIT. These results were the same for homo sapiens and

**Table 1.** Changes in body weight and blood glucose values of rats before and after STZ administration

Groups	Bodyweight (g)		Blood glucose (mg/dL)	
	First	After 6 weeks	First	After 6 weeks
Control	346.3 $\pm$ 11.6	358.8 $\pm$ 7.7	93.80 $\pm$ 2.01	96.88 $\pm$ 1.64
Diabetes	371.9 $\pm$ 5.08	271.5 $\pm$ 6.32*	98.99 $\pm$ 1.81	471.48 $\pm$ 30.26*

Data are presented as mean  $\pm$  standard deviation, \* $p < 0.001$ , different according to the first application in the diabetes group, † $p < 0.001$ , different according to the control group. STZ: Streptozotocin

**Table 2.** miRNA fold changes according to microarray analysis

miRNAs	Fold change	Accession numbers	Primer sequences
rno-miR-200c-3p	4.15	MIMAT000873	TAATACTGCCGGTAATGATG
rno-miR-129-5p	3.89	MIMAT000600	CTTTTTCGGTCTGGGCTTGC
rno-miR-150-3p	3.82	MIMAT0017133	CTGGTACAGGCCTGGGA
rno-miR-3584-5p	3.55	MIMAT0017875	GGGAGGAGTCCAGGAGGC
rno-miR-34c-3p	-7.02	MIMAT0004723	AATCACTAACCACACAGCCAGG
rno-miR-342-3p	-8.07	MIMAT0000589	TCTCACACAGAAATCCACCCGT
rno-miR-466b-3p	-36.47	MIMAT0017285	ATACATACACACACATACAC
rno-miR-466c-3p	-9.58	MIMAT0017287	TATACATGCACACATACAC
rno-miR-31a-3p	-9.72	MIMAT0000810	AGCAAGATGCTGGCATAGCTG
rno-miR-15b-5p	-9.9	MIMAT0000784	TAGCAGCATCATGGTTTACA
rno-miR-196b-3p	-19.37	MIMAT0017171	TCGACAGCAGCAGACTCCTTCA
rno-miR-208a-5p	-60.8	MIMAT0017155	GAGCTTTTGCCCGGGTTATAAC

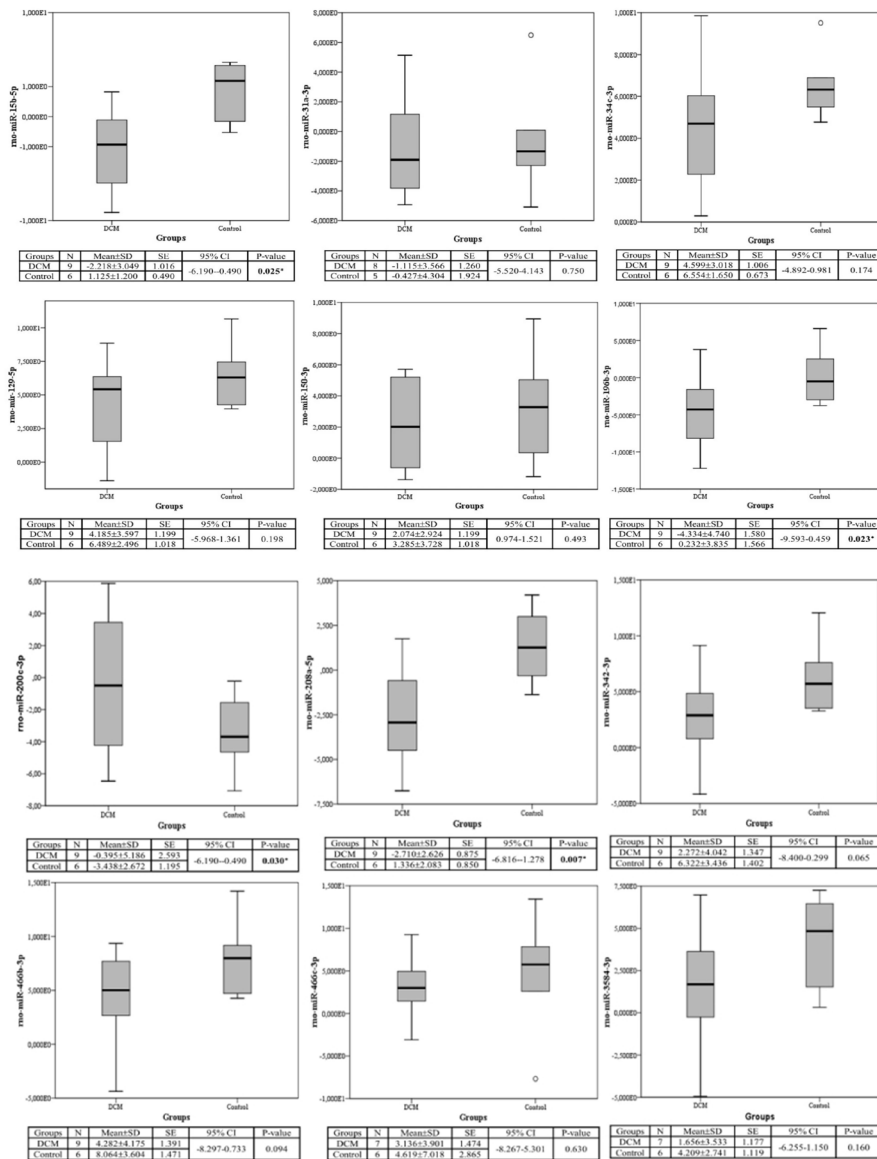


**Figure 1.** miRNA expression differences diabetes and control groups

Mus musculus (miRNAs have a high degree of seed sequence homology for both species). KEGG pathway analysis showed that the *GRAP2* gene (K07366) was primarily effective in the T-cell receptor signaling pathway. Two signaling pathways were featured in this study: Calcium signaling (nt06120) and TGR-NFAT signaling pathway (N01106). The results were checked in the Reactome database and it was determined that the *GRAP2* gene was effective in the secondary messenger system. The cellular localization of GRAP2 was shown to be cytoplasm, cytosol, endosome, nucleoplasm, nucleus, and plasma membrane. It was determined that GRAP2 was highly expressed in the heart and pericardium and its molecular function is protein binding (Figure 3) (Reactome) (18). In our analysis to determine which of the four miRNAs targeting the same gene could bind primarily, miR-200c-3p had a high degree of target activity, while the other

3 miRNAs (miR-15b-5p, miR-196b-3p, and miR-208a-5p) were found to have moderate target efficiency.

**ROC Curve Analysis**

In the ROC analysis for four miRNAs, miR-200c-3p had the potential to be biomarkers (p<0.05) (Table 4, Figure 4), and heart tissue miRNAs were expressed differently in DCM. In addition, this miRNA was thought to be associated with the DCM.

**Histopathological Analysis**

Myocyte diameters were measured in each of the sections taken from six different heart tissues obtained from the control group (16.35±0.66) and nine different heart tissues obtained from the

**Table 3.** miRNA fold change and regulation status according to expression analysis

miRNAs	Diabetes (fold change)	Regulation
rno-miR-200c-3p	16.56	Upregulated
rno-miR-129-5p	4.93	Upregulated
rno-miR-150-3p	0.23	Upregulated
rno-miR-3584-5p	5.86	Upregulated
rno-miR-34c-3p	3.87	Downregulated
rno-miR-342-3p	0.22	Downregulated
rno-miR-466c-3p	3.81	Downregulated
rno-miR-31a-3p	1.61	Downregulated
rno-miR-15b-5p	10.14	Downregulated
rno-miR-196b-3p	23.70	Downregulated
rno-miR-466b-3p	3.75	Downregulated
rno-miR-208a-5p	16.53	Downregulated

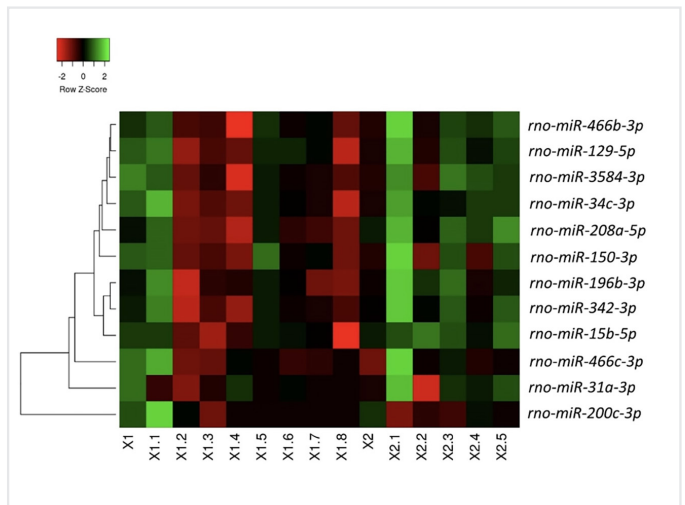


**Figure 2.** The Heatmap differentially expression of miRNAs. Average linkage and spearman rank correlation were used in the analysis of the data. X1-X1.8; diabetes group, X2-X2.5; control group

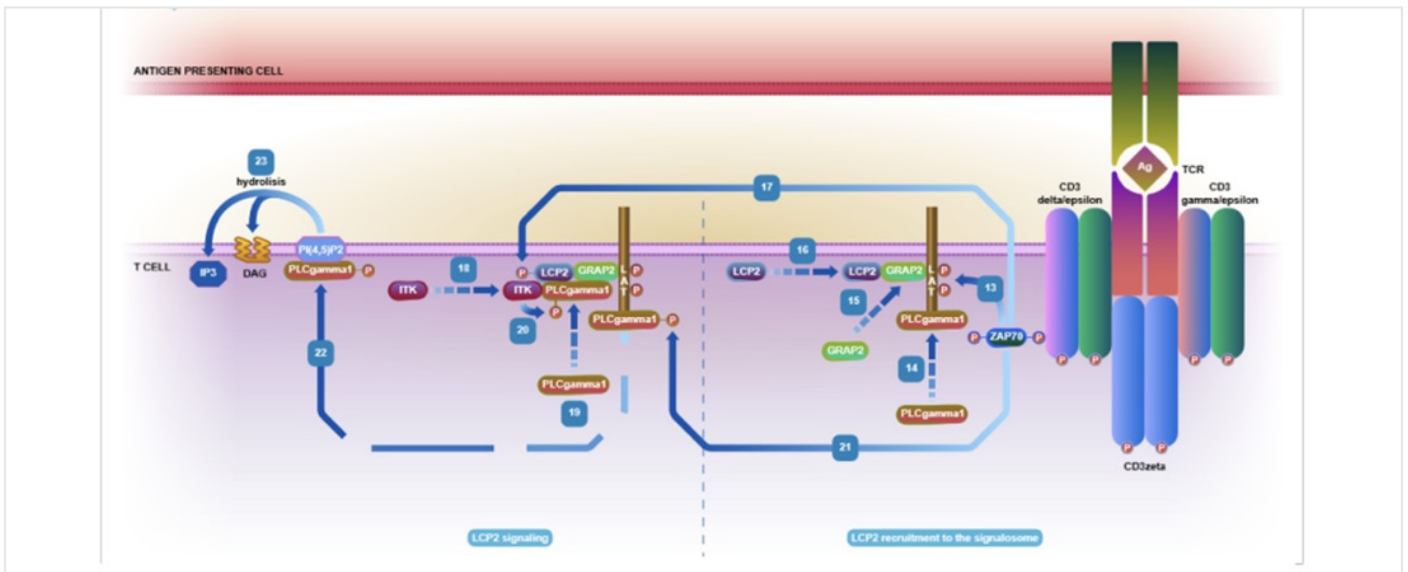


**Figure 3.** GRAP2 function in T-cell  
*GRAP2: GRB2-related adapter protein 2*

diabetes group ( $31.45 \pm 0.74$ ) group. The mean myocyte diameter in diabetes was found to be high ( $p < 0.05$ ). Additionally, hypertrophic cardiomyocytes were found in the ventricular region of rats in the diabetes group (Figure 5C, D, E, F) and cardiomyocytes showing pale acidophilic staining in these regions were also remarkable (Figure 5D). Occasional vacuolization was observed in some cardiomyocytes (Figure 6D). In the diabetes group, more intense connective tissue staining and increased interstitial cardiac fibrosis were observed (Figure 6E, F).

### Discussion

Diabetes mellitus is a progressive, chronic, and metabolic disease characterized by hyperglycemia and glycosuria, which develops due to insufficient insulin secretion in the pancreas and/or insufficient response of tissues to insulin (19). Controlling hyperglycemia significantly decreases diabetes-related mortality rates and acute complications (20).

The incidence of morbidity and mortality in diabetic patients increases with complications (21). Increased levels of free radicals contribute to the development of diabetes complications by causing oxidation-related cell damage in many tissues, especially the endothelium (22). Type 1 and type 2 diabetes are primary risk factors for cardiovascular diseases (23). Studies have reported that miRNAs regulate cardiomyocyte hypertrophy, myocardial fibrosis, cardiomyocyte apoptosis, mitochondrial dysfunction, myocardial electrical remodeling, epigenetic modification, and

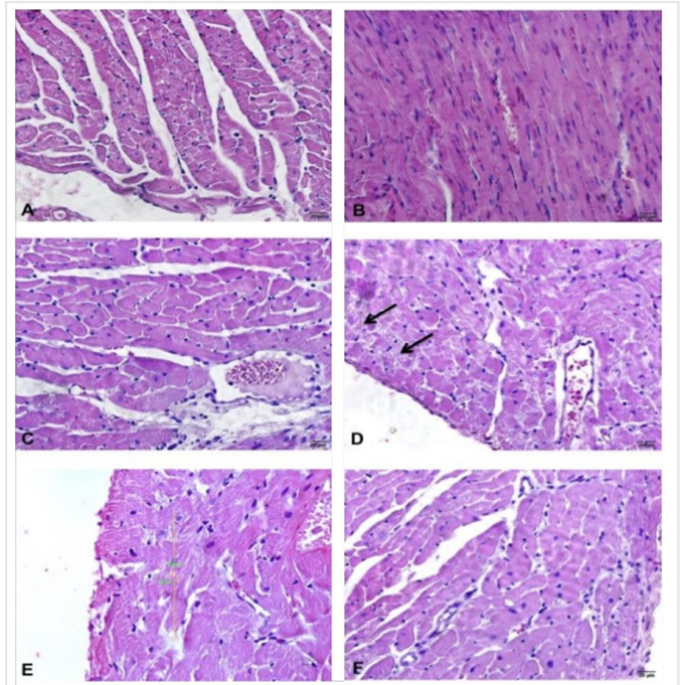


**Figure 5.** Hematoxyline and eosin staining in control and diabetes samples of myofibril

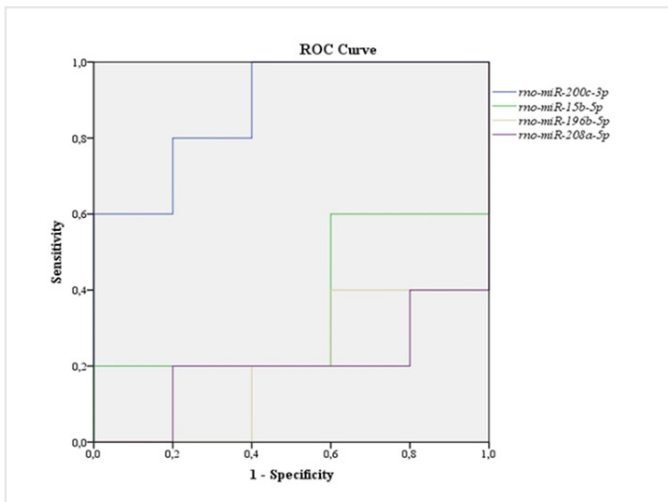


**Figure 4.** Comparison of sensitivity and specificity of the four miRNAs diabetes and control groups

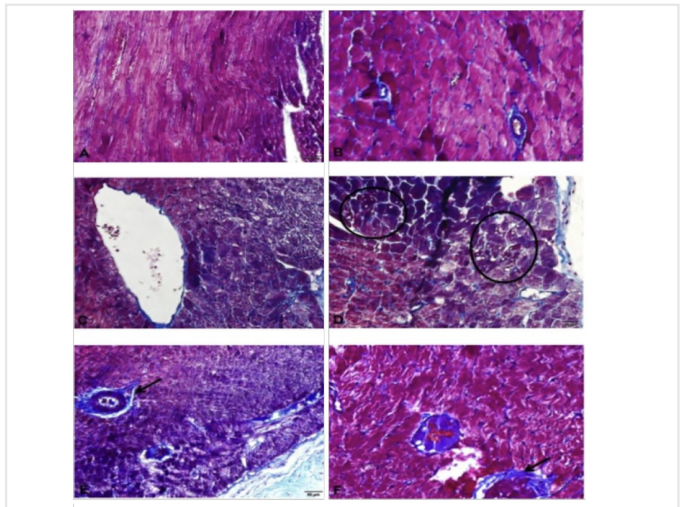


**Figure 6.** Hematoxyline and eosin staining in control and diabetes samples for cardiomyocyte hypertrophy

**Table 4.** ROC curve analysis of four miRNAs for control and diabetes groups

Compared groups	Tissue	Test variables	AUC	95% CI	p-value	Specificity	Sensitivity	Criterion
Diabet versus control	Heart	rno-miR-200c-3p	0.815	[0.535-0.963]	0.018	77.78	83.33	>27.70
		rno-miR-15b-5p	0.537	[0.269-0.790]	0.823	22.22	100	>23.28
		rno-miR-196b-3p	0.630	[0.349-0.857]	0.394	66.70	66.70	≤29.00
		rno-miR-208a-5p	0.611	[0.333-0.844]	0.492	77.78	50	≤27.13

AUC: Area under the curve, CI: Confidence interval, ROC: Receiver operating characteristic

various other pathophysiological processes (24). Additionally, the expression levels of DCM-related miRNAs affect the pathophysiology of the diabetes (25).

miRNA expression levels change similarly in cardiac pathologies such as cardiac hypertrophy, heart failure, and myocardial infarction (26). The cardiac expression of miR-200c is significantly upregulated in diabetic rats (27). miR-200c has specific activity on the functions of dual-specificity phosphatase-1 (DUSP-1), a MAPK phosphatase that regulates the phosphorylation of p-ERK, p-JNK, and p-p38. The expression of miR-200c is high in this model. miR-200c inhibition reduces cardiac hypertrophy by activating DUSP-1 in cardiomyocytes in the diabetes model. In another study, the downregulation of miR-200c protects cardiomyocytes from apoptosis due to hypoxia (28). In our study, miR-200c-3p was upregulated. It can be thought that the upregulation of miR-200c is associated with DCM pathology.

It is reported that Sp1-mediated matrix metalloproteinase-9 (MMP-9) expression plays an important role in diabetic wound healing. miR-129 and miR-335 are known to inhibit MMP-9 expression by targeting Sp1 (29). These two miRNAs upregulated lead to MMP-9 downregulation, which in turn promotes wound healing. There are no studies on the expression of this miRNA in DCM. However, computational studies have shown that miR-129 is upregulated during heart failure (30). Our results showed that the upregulation of miR-129a-5p might be involved in the DCM process, although it was not statistically significant.

In a hypertension model in rats, miR-3584 was reported to be upregulated (31). In another study, miR-3584 was upregulated in plasma in patients with pulmonary arterial hypertension (32).

A study indicated that 19 miRNAs in C2C12 myotubes regulated mitochondrial metabolism in skeletal muscle.

Four of these miRNAs (miR-34c-3p, miR-150-5p, miR-196b-3p, and miR-320a) were reported to be associated with skeletal muscle mitochondrial function in humans (33). Another study found that miR-34c was overexpressed and suppressed in hypertrophic cardiomyopathy, resulting in improved cardiac function (34). In our study, miRNA-34c and miRNA-196b expressions were downregulated, and miR-150 expression was upregulated. Therefore, it can be thought that miR-34c and miR-196b have a triggering role in the pathogenesis of DCM.

miR-15 is dysregulated in cardiovascular and neurological diseases (35). Dysregulation of miR-15b has been shown to cause ROS generation, which controls ATP production, leading to heart disease (35). In our study, miR-15b expression was shown to be downregulated. Contrary to these studies, miR-15b-5p targets the 5' untranslated (UTR) regions of genes. The 3' and 5' regions in the gene have different functions. 5' UTRs are important in gene regulation by miRNAs as they are translational control regions of gene expression. Thus, the stability of the gene can be checked (36). Since a miRNA can target more than one gene, tissue-specific miRNAs have a fundamental role in demonstrating their activity in diseases (37). The expression of this miRNA in the cardiac tissue is high and our results show that its expression

in DCM is quite high compared to the controls (Fold change =10.14). miR-15b-5p can be an epigenetic regulator in the pathology of DCM.

The target genes of miR-466-3p are transcription factors and kinases that are actively involved in cell cycle, apoptosis and other cellular events (38). miR-466-3p is thought to be responsible for lung and breast cancer and cardiovascular system diseases. miR-466 may play an important role in DCM as it affects proteins known to be closely associated with inflammation. In our study, miR-466 was downregulated and this miRNA might play a role in the pathogenesis of DCM.

miRNA analyses were performed in rat cardiomyocytes on postnatal day 0 and day 10 (39). miR-31a-5p expression increased on the 10<sup>th</sup> day in isolated cardiomyocytes and this increase terminated the cell cycle. However, it is unclear how miR-31a-5p affects mature cardiomyocyte proliferation. miR-31a-5p is a negative modulator in the cardiac fibrogenic epithelial-mesenchymal transition of epicardial mesothelial cells. miR-31a-5p was found to be specifically increased in human atrial fibrillation; this was thought to cause loss of atrial dystrophin and neuronal nitric oxide synthase (40).

In our study, the downregulation of miR-31a-5p was also detected. The opposite of the results reported in previous studies could be explained by the presence of a possible compensatory mechanism. In this way, it may be aimed to increase dystrophin and neuronal nitric oxide synthase levels in response to the development of cardiomyopathy. Another study on atheromatous plaques suggested that miR-31 had an anti-inflammatory effect. Therefore, the downregulation of miR-31a-5p in our study can be explained by the fact that inflammation is one of the main factors in cardiomyopathy. miR-31a-5p plasma level was significantly decreased in heart failure patients compared to healthy volunteers (41). Our results are similar to this study.

In miR-208a silenced mice, the loss of miR-208a caused significant expression of multiple skeletal muscle contractile protein genes that were not normally expressed in the heart (42). In our study, it was thought that downregulation of miR-208a was a compensatory mechanism that develops against the pathogenesis of cardiomyopathy. Also, miR-208a is released from damaged cardiomyocytes in the bloodstream. The increased levels of miR-208a may be an important marker in the diagnosis of DCM. Similarly, in a study with mice, it was found that the plasma concentration of miR-208-a increased in myocardial damage and showed a significant correlation with cardiac troponin plasma concentration, and this might be an important indicator of myocardial damage (43,44).

Considering the histopathological results; in the control group, the nuclei of the heart muscle cells were centrally located, their cytoplasm was pale and the intercalated disc was normal. Hydropic degeneration, increase in nuclear size, and occasional vesiculation were observed in myocytes in the diabetes group. Additionally, trichrome staining revealed mild to moderate fibrosis in the interstitial area. Different studies have shown that different miRNAs

are involved in the pathogenesis of cardiomyocyte hypertrophy in DCM (45-49). One of the main features of DCM is cardiac fibrosis and its cause is excessive accumulation of extracellular matrix proteins. In diabetic heart tissue, miRNA regulation may occur under the influence of diabetes. It is inevitable to regulate fibrosis through signaling pathways in cardiac endothelial cells, fibroblasts and myocytes. miRNA dysregulation is associated with structural changes in cardiac tissue.

miR-150 expression level was significantly decreased in cardiomyocyte hypertrophy (45). In our study, cardiomyocyte hypertrophy was observed in the diabetes group, consistent with the results of this study. In another study, degenerative changes were reported in the STZ-induced diabetes model (50). In other studies, the intracellular pH level decreases with acidosis of the cell, and multiple enzyme activities occur (51). Basic groups are given to the environment by the denaturing of the structural and enzymatic cytoplasm proteins by activated enzymes showing affinity to acid dyes (eosin), causing acidophilic staining of the cytoplasm (52). In our study, pale acidophilic staining was observed in diabetic rats. In the STZ-induced diabetes model, there was minimal change in ventricular muscle cells in the 8-10-week period in rats (53).

Where more than one miRNA targets a single gene, free energy and sequence specificity may indicate that the miRNA is efficiently bound (54). In our study, we determined the conservation of miRNAs with the target gene, GRAP2, using TargetScan. miR-200c-3p has a higher probability of matching than other miRNAs. It is predicted that the pathological effects of GRAP2, which is regulated by these 4 miRNAs, on DCM are realized in T-cell signaling. In DCM, cytokines and chemokines are secreted by inflammatory cells in the heart tissue. These substances cause the development of cardiomyocyte hypertrophy and remodeling of the extracellular matrix. This activation triggers the release of several cytokines by affecting various inflammatory cells and cardiac damage is induced. In STZ-induced mice, the myocardium has a higher T-cell infiltration (55).

### Study Limitations

The expression level of the *GRAP2* gene, which is the target gene of miR-200c-3p, can be examined.

### Conclusion

The *GRAP2* gene may play a role in the T-cell receptor function of miRNAs and that their downregulation may contribute to the pathology of DCM. GRAP2 expression can be examined. It is also possible that miR-200c-3p can be used as epigenetic regulators or biomarkers in DCM.

### Ethics

**Ethics Committee Approval:** Ethics committee approval is not required.

**Informed Consent:** Informed consent is not required.

### Footnotes

#### Authorship Contributions

Surgical and Medical Practices: A.Ş.D., M.P., A.B., H.K.E., Concept: M.P., H.K.E., Design: M.P., Ş.G.Y., H.K.E., Data Collection or Processing: M.P., Analysis or Interpretation: M.P., Ş.G.Y., A.K., Y.P., H.K.E., Literature Search: A.Ş.D., M.P., Writing: M.P., Ş.G.Y., H.K.E.

**Conflict of Interest:** No conflict of interest was declared by the authors.

**Financial Disclosure:** The authors declared that this study received no financial support.

### References

- Jia G, Hill MA, Sowers JR. Diabetic cardiomyopathy: an update of mechanisms contributing to this clinical entity. *Circ Res*. 2018;122:624-38.
- Felício JS, Koury CC, Carvalho CT, Abrahão Neto JF, Miléo KB, Arbage TP, et al. Present insights on cardiomyopathy in diabetic patients. *Curr Diabetes Rev*. 2016;12:384-95.
- Jia G, Whaley-Connell A, Sowers JR. Diabetic cardiomyopathy: a hyperglycaemia- and insulin-resistance-induced heart disease. *Diabetologia*. 2018;61:21-8.
- Obokata M, Reddy YNV, Borlaug BA. Diastolic dysfunction and heart failure with preserved ejection fraction: understanding mechanisms by using noninvasive methods. *JACC Cardiovasc Imaging*. 2020;13:245-57.
- Ghosh N, Katare R. Molecular mechanism of diabetic cardiomyopathy and modulation of microRNA function by synthetic oligonucleotides. *Cardiovasc Diabetol*. 2018;17:43.
- Ritchie RH, Abel ED. Basic mechanisms of diabetic heart disease. *Circ Res*. 2020;126:1501-25.
- Chandramouli C, Reichelt ME, Curl CL, Varma U, Bienvenu LA, Koutsifeli P, et al. Diastolic dysfunction is more apparent in STZ-induced diabetic female mice, despite less pronounced hyperglycemia. *Sci Rep*. 2018;8:2346.
- Wang S, Ding L, Ji H, Xu Z, Liu Q, Zheng Y. The role of p38 MAPK in the development of diabetic cardiomyopathy. *Int J Mol Sci*. 2016;17:1037.
- Watanabe K, Thandavarayan RA, Harima M, Sari FR, Gurusamy N, Veeraveedu PT, et al. Role of differential signal-ing pathways and oxidative stress in diabetic cardiomyopathy. *Curr Cardiol Rev*. 2010;6:280-90.
- Silva DCPD, Carneiro FD, Almeida KC, Fernandes-Santos C. Role of miRNAs on the pathophysiology of cardiovascular diseases. *Arq Bras Cardiol*. 2018;111:738-46.
- O'Brien J, Hayder H, Zayed Y, Peng C. Overview of MicroRNA biogenesis, mechanisms of actions, and circulation. *Front Endocrinol (Lausanne)*. 2018;9:402.
- Zhang S, Weinheimer C, Courtois M, Kovacs A, Zhang CE, Cheng AM, et al. The role of the Grb2-p38 MAPK signaling pathway in cardiac hypertrophy and fibrosis. *J Clin Invest*. 2003;111:833-41.

13. Manu MS, Rachana KS, Advirao GM. Altered expression of IRS2 and GRB2 in demyelination of peripheral neurons: Implications in diabetic neuropathy. *Neuropeptides*. 2017;62:71-9.
14. Akbarzadeh A, Norouzian D, Mehrabi MR, Jamshidi SH, Farhangi A, Allah Verdi A, et al. Induction of diabetes by streptozotocin in rats. *Indian J Clin Biochem*. 2007;22:60-4.
15. Masè M, Grasso M, Avogaro L, D'Amato E, Tessarolo F, Graffigna A, et al. Selection of reference genes is critical for miRNA expression analysis in human cardiac tissue. A focus on atrial fibrillation. *Sci Rep*. 2017;7:41127.
16. Livak KJ, Schmittgen TD. Analysis of relative gene expression data using real-time quantitative PCR and the 2(-Delta Delta C(T)) Method. *Methods*. 2001;25:402-8.
17. Kiernan JA. *Histological and histochemical methods: theory and practice*, 3rd edition. Shock. 1999;12:479.
18. Fabregat A, Korninger F, Viteri G, Sidiropoulos K, Marin-Garcia P, Ping P, et al. Reactome graph database: Efficient access to complex pathway data. *PLoS Comput Biol*. 2018;14:e1005968.
19. American Diabetes Association. Diagnosis and classification of diabetes mellitus. *Diabetes Care*. 2014;37(Suppl 1):81-90.
20. Sherwani SI, Khan HA, Ekhzaimy A, Masood A, Sakharkar MK. Significance of HbA1c test in diagnosis and prognosis of diabetic patients. *Biomark Insights*. 2016;11:95-104.
21. Chawla A, Chawla R, Jaggi S. Microvascular and macrovascular complications in diabetes mellitus: Distinct or continuum? *Indian J Endocrinol Metab*. 2016;20:546-51.
22. Öztürk Z. Diabetes, oxidative stress and endothelial dysfunction. *Bezmialem Science*. 2019;7:52-7.
23. Einarson TR, Acs A, Ludwig C, Panton UH. Prevalence of cardiovascular disease in type 2 diabetes: a systematic literature review of scientific evidence from across the world in 2007-2017. *Cardiovasc Diabetol*. 2018;17:83.
24. Huang ZP, Neppel RL, Wang DZ. MicroRNAs in cardiac remodeling and disease. *J Cardiovasc Transl Res*. 2010;3:212-8.
25. Felekis K, Papanephytou C. Challenges in using circulating biomarkers for cardiovascular diseases. *Int J Mol Sci*. 2020;21:561.
26. Mir R, Elfaki I, Khullar N, Waza AA, Jha C, Mir MM, et al. Role of selected miRNAs as diagnostic and prognostic biomarkers in cardiovascular diseases, including coronary artery disease, myocardial infarction and atherosclerosis. *J Cardiovasc Dev Dis*. 2021;8:22.
27. Singh GB, Raut SK, Khanna S, Kumar A, Sharma S, Prasad R, et al. MicroRNA-200c modulates DUSP-1 expression in diabetes-induced cardiac hypertrophy. *Mol Cell Biochem*. 2017;424:1-11.
28. Chen Z, Zhang S, Guo C, Li J, Sang W. Downregulation of miR-200c protects cardiomyocytes from hypoxia-induced apoptosis by targeting GATA-4. *Int J Mol Med*. 2017;39:1589-96.
29. Wang W, Yang C, Wang XY, Zhou LY, Lao GJ, Liu D, et al. MicroRNA-129 and -335 promote diabetic wound healing by inhibiting Sp1-Mediated MMP-9 expression. *Diabetes*. 2018;67:1627-38.
30. Thum T, Galuppo P, Wolf C, Fiedler J, Kneitz S, van Laake LW, et al. MicroRNAs in the human heart: a clue to fetal gene reprogramming in heart failure. *Circulation*. 2007;116:258-67.
31. Sun G, Hu H, Tian X, Yue J, Yu H, Yang X, et al. Identification and analysis of microRNAs in the left ventricular myocardium of two-kidney one-clip hypertensive rats. *Mol Med Rep*. 2013;8:339-44.
32. Yang Y, Li R, Cao Y, Dai S, Luo S, Guo Q, et al. Plasma MIR-212-3p as a biomarker for acute right heart failure with pulmonary artery hypertension. *Ann Transl Med*. 2020;8:1571.
33. Dahlmans D, Houzelle A, Andreux P, Jörgensen JA, Wang X, de Windt LJ, et al. An unbiased silencing screen in muscle cells identifies miR-320a, miR-150, miR-196b, and miR-34c as regulators of skeletal muscle mitochondrial metabolism. *Mol Metab*. 2017;6:1429-42.
34. Bernardo BC, Gao XM, Tham YK, Kiriazis H, Winbanks CE, Ooi JY, et al. Silencing of miR-34a attenuates cardiac dysfunction in a setting of moderate, but not severe, hypertrophic cardiomyopathy. *PLoS One*. 2014;9:e90337.
35. Zheng M, Wang M. A narrative review of the roles of the miR-15/107 family in heart disease: lessons and prospects for heart disease. *Ann Transl Med*. 2021;9:66.
36. Gu W, Xu Y, Xie X, Wang T, Ko JH, Zhou T. The role of RNA structure at 5' untranslated region in microRNA-mediated gene regulation. *RNA*. 2014;20:1369-75.
37. Peter ME. Targeting of mRNAs by multiple miRNAs: the next step. *Oncogene*. 2010;29:2161-4.
38. Niyazova R, Atambayeva Sh, Akimniyazova A, Pinsky I, Alybaeva A, Faye B, et al. Features of mir-466-3p binding sites in mRNA genes with different functions. *Int J Biol Chem*. 2015;8:44-51.
39. Xiao J, Liu H, Cretoiu D, Toader DO, Suci N, Shi J, et al. miR-31a-5p promotes postnatal cardiomyocyte proliferation by targeting RhoBTB1. *Exp Mol Med*. 2017;49:e386.
40. Reilly SN, Liu X, Carnicer R, Recalde A, Muszkiewicz A, Jayaram R, et al. Up-regulation of miR-31 in human atrial fibrillation begets the arrhythmia by depleting dystrophin and neuronal nitric oxide synthase. *Sci Transl Med*. 2016;8:340-74.
41. Ellis KL, Cameron VA, Troughton RW, Frampton CM, Ellmers LJ, Richards AM. Circulating microRNAs as candidate markers to distinguish heart failure in breathless patients. *Eur J Heart Fail*. 2013;15:1138-47.
42. van Rooij E, Sutherland LB, Qi X, Richardson JA, Hill J, Olson EN. Control of stress-dependent cardiac growth and gene expression by a microRNA. *Science*. 2007;316:575-9.
43. Jaffe AS, Ravkilde J, Roberts R, Naslund U, Apple FS, Galvani M. It's time for a change to a troponin standard. *Circulation*. 2000;102:1216-20.
44. Ji X, Takahashi R, Hiura Y, Hirokawa G, Fukushima Y, Iwai N. Plasma miR-208 as a biomarker of myocardial injury. *Clin Chem*. 2009;55:1944-9.
45. Duan Y, Zhou B, Su H, Liu Y, Du C. miR-150 regulates high glucose-induced cardiomyocyte hypertrophy by targeting the transcriptional co-activator p300. *Exp Cell Res*. 2013;319:173-84.
46. Feng B, Chen S, George B, Feng Q, Chakrabarti S. miR133a regulates cardiomyocyte hypertrophy in diabetes. *Diabetes Metab Res Rev*. 2010;26:40-9.
47. Kuwabara Y, Horie T, Baba O, Watanabe S, Nishiga M, Usami S, et al. MicroRNA-451 exacerbates lipotoxicity in cardiac myocytes

- and high-fat diet-induced cardiac hypertrophy in mice through suppression of the LKB1/AMPK pathway. *Circ Res.* 2015;116:279-88.
48. Raut SK, Kumar A, Singh GB, Nahar U, Sharma V, Mittal A, et al. miR-30c mediates upregulation of Cdc42 and Pak1 in diabetic cardiomyopathy. *Cardiovasc Ther.* 2015;33:89-97.
49. Shen E, Diao X, Wang X, Chen R, Hu B. MicroRNAs involved in the mitogen-activated protein kinase cascades pathway during glucose-induced cardiomyocyte hypertrophy. *Am J Pathol.* 2011;179:639-50.
50. Yan B, Ren J, Zhang Q, Gao R, Zhao F, Wu J, et al. Antioxidative effects of natural products on diabetic cardiomyopathy. *J Diabetes Res.* 2017;2017:2070178.
51. Cai F. [Studies of enzyme histochemistry and ultrastructure of the myocardium in rats with streptozotocin-induced diabetes]. *Zhonghua Yi Xue Za Zhi.* 1989;69:276-8.
52. Miller MA, Zavhary JF. Mechanisms and morphology of cellular injury, adaptation, and death. *Pathologic Basis of Veterinary Disease.* 2017:2-43.
53. Zhang J, Qiu H, Huang J, Ding S, Huang B, Wu Q, et al. Establishment of a diabetic myocardial hypertrophy model in *Mus musculus castaneus* mouse. *Int J Exp Pathol.* 2018;99:295-303.
54. Witkos TM, Koscianska E, Krzyzosiak WJ. Practical aspects of microRNA target prediction. *Curr Mol Med.* 2011;11:93-109.
55. Tan Y, Zhang Z, Zheng C, Wintergerst KA, Keller BB, Cai L. Mechanisms of diabetic cardiomyopathy and potential therapeutic strategies: preclinical and clinical evidence. *Nat Rev Cardiol.* 2020;17:585-607.
- 

**Supplementary link:** <https://l24.im/MtgRL>